University of Thessaly

Department of Mechanical Engineering

Diploma Thesis

EFFECT OF THERMAL PROCESS ON CORROSION BEHAVIOUR OF ALUMINIUM-CONTAINING TRIP 700 STEEL

by

PATROKLOS SARIGIOVANNIS

SUBMITTED IN PARTIAL FULFILLMENT OF THE

REQUIREMENTS FOR THE DIPLOMA IN MECHANICAL ENGINEERING

2017

Examined by the following members of the Advisory Committee:

First Member (Supervisor)

Alexis Kermanidis
Assistant Professor of Mechanical Behaviour of Materials,
Department of Mechanical Engineering, University of Thessaly

Second Member

Vasileios Bontozoglou
Professor of Transport Phenomena,
Department of Mechanical Engineering, University of Thessaly

Third Member

Dr Anna Zervaki
Laboratory Teaching Staff,
Department of Mechanical Engineering, University of Thessaly

Abstract

The present study focuses primarily on the possible effects of certain thermal processes on the corrosion characteristics of TRIP steels containing aluminium. In the investigation 4 TRIP materials were used, based on a TRIP 700 Al-containing steel, with differences in microstructure due varying heat treatment parameters in the isothermal bainitic transformation region. The corrosion behavior of the TRIP steels is investigated following immersion of samples in 3.5% NaCl solution. After removal of the samples from the corrosive medium, characteristic corrosion parameters were evaluated using optical microscopy, such as mass variation and size of corrosion pits. The differences in corrosion behavior observed in the materials are discussed taking into account microstructural characteristics of the investigated steels.

Nomenclature

γ_R	retained austenite
γ	austenite
α'	martensite
a	ferrite
α_B	bainite
A_{C1}	temperature of austenitisation initiation
A_{C3}	temperature of austenitisation completion
BCC	Body-Centered Cubic
FCC	Face-Centered Cubic
SEM	Scanning Electron Microscopy
IBT	Isothermal Bainitic Transformation
IA	Intercritical Annealing

Acknowledgements

First and foremost I would like to thank the supervisor of my thesis, Assistant Professor Alexis Kermanidis for his eagerness to navigate my research to issues I would have never considered myself before and for all his help and instruction during the creation of this thesis. I am also very grateful to Professor Gregory Haidemenopoulos for permitting me to use the equipment of his laboratory and offering useful information and all the teaching and technical staff of the Laboratory of Materials for their guidance and their valuable advice, through which I managed to greatly improve the quality of my research. I especially thank Mrs Kamoutsi for her enduring interest and assistance in various matters throughout my undergraduate studies and her special help with many technical issues. A great deal of credit should also go to Mr Athanasios Vergos, who was extremely helpful with the machining and cutting procedures. Furthermore, I would like to thank Voestalpine for providing the high quality material that was used in the experiments. Lastly, I thank all my friends and family who inspired my path up to here.

Table of Contents

1. Introduction

The ever evolving demands to reduce CO_2 emissions has focused the attention of automotive industries and steel manufacturers on the development and application of new, advanced high strength steels (HSS) with high formability allowing for the design of lighter vehicles through the manufacturing of components featuring complex geometries with reduced thickness. Among the HSS, *Transformation Induced Plasticity* (TRIP) *Steels*, which were discovered in the 1960s by Zackay *et al.* [1], exhibit an excellent combination of strength and formability compared to solid solution steels and DP steels.

Further research focused on TRIP steels has been directed to various of their possible exploitable properties. Effect of alloying elements like manganese [2] and silicon [3] and tests of the mechanical strength and elasticity of TRIP steels are common examples of research referring to such steels, and even their suitability for forming processes has been studied. Further investigation of their long term behaviour in order to increase their potential application in the automotive industry should aim to a careful characterisation of their corrosion properties, which hare linked to their processing parameters and microstructural characteristics.

The primal idea behind the present thesis is an interest to investigate how the heat treatment process could influence the characteristics of corrosion in an Al-containing TRIP 700 steel, through the modification of their microstructure. For this purpose, the corrosion behavior was investigated under laboratory conditions, simulating corrosion processes occurring in natural environment. A study focused on sea conditions would be useful to the elucidation of the suitability of such alloys for both marine structures and vessels and also land

applications interacting with seawater in various forms. With TRIP steels being often promoted chiefly as a material suited for automobile cars due to their formability, there was a driving force to examine potential suitability of those steels for marine and sea-affected environments as well, which create different ambient conditions.

Existing publications have noted the significance of the martensitic and the bainitic phases related to the behaviour of multiphase steels against corrosion and demonstrated that that non-equilibrium phases like martensite and bainite appear in general more prone to corrosion and act as anodic phases. [4]

Motivated by the complex and innovative microstructure of TRIP steels and taking into consideration that the fair majority of academic papers devoted to the corrosion of TRIP steels have turned their attention towards potentiodynamic polarisation tests [5], SEM micrographs [6] and electrochemical issues, there was an incentive to approach the subject through the examination of the characteristics of surface and microstructure by more practical and primary methods.

To reproduce conditions representative of the original seawater conditions, a solution of 3,5 wt% sodium chloride (NaCl) in deionised water the ASTM G44 was followed. The aim was to observe the effect of the saline water environment on the characteristic sizes of pitting corrosion in TRIP 700 steel specimens under different heat treatment conditions. Afterwards, the research proceeded with the visual inspection of corroded samples via optical microscopy and statistical calculations based on microscopic results. Conclusions were then based on these data.

2. Theoretical Overview

2.1 Corrosion theory

2.1.1 General overview

Corrosion constitutes one of the biggest problems of metallic structures since it is linked with aspects of material degradation and structural integrity. It involves the gradual degeneration of materials through the reaction with its environment and the formation of oxides.

Corrosion types can be divided into many categories based on the appearance of the corrosion damage or the mechanism of attack, prominent among which are:

Uniform or *general corrosion*, which, as the name implies, results in a fairly uniform penetration or thinning over the entire exposed metal surface. The general attack results from local corrosion cell action; this means that multiple anodes and cathodes are active on the metal surface at any given time. The location of the anodic and cathodic areas continues to move about the surface, resulting in uniform corrosion. General corrosion inflicts the greatest destruction of metal on a tonnage basis.

Crevice corrosion, which is a type of localised attack that occurs at narrow openings or spaces (gaps) between metallic components or between a non-metallic and a metallic surface. This type of corrosion is the result of a concentration cell formed between the electrolyte within the crevice, which has a deficiency of oxygen, and the electrolyte outside the crevice, where oxygen is more abundant. The material within the crevice acts as the anode, and the exterior material becomes the cathode.

Erosion-corrosion, which constitutes a complex type of attack due to the acceleration in the rate of deterioration or attack on a metal because of mechanical wear or abrasive contributions in combination with corrosion. Such a combination results in more severe degeneration than either mechanical or chemical corrosive action alone. Metal is removed from the surface in the form of dissolved ions, particles of solid corrosion products, or elemental metal. The spectrum of erosion-corrosion ranges from types of primarily erosive attack, such as sandblasting, filing, or grinding of a metal surface, to primarily corrosive failure where the contribution of mechanical action is quite limited. Common examples of erosion-corrosion include relative movement between a corrosive fluid and a metallic surface, cavitation and fretting corrosion. Erosion-corrosion is characterized in appearance by grooves, waves, rounded holes, and/or horseshoe-shaped grooves.

Intergranular corrosion, defined as the selective dissolution of grain boundaries, or closely adjacent regions, without significant attack against the grains themselves. This dissolution is caused by differences in voltage potential between the grain-boundary region and any precipitates, intermetallic phases, or impurities that form at the grain boundaries. The actual mechanism differs with each alloy system. Precipitates that form as a result of the exposure of metals at elevated temperatures (for example, during production, fabrication, and welding) often nucleate and grow preferentially at grain boundaries. If these precipitates are rich in alloying elements that are essential for corrosion resistance, the regions adjacent to the grain boundary are depleted of these elements.

Exfoliation is a form of intergranular corrosion that primarily affects aluminum alloys in industrial or marine environments. Corrosion proceeds laterally from initiation sites on the surface and generally proceeds along grain boundaries, on planes parallel to the surface. The corrosion products formed on the grain boundaries force metal to split away from the underlying base material, resulting in a layered or flake-like appearance.

2.1.2 Pitting Corrosion

Pitting constitutes an extremely localised form of corrosion that produces sharply defined holes. These holes may feature a small or large diameter, but most usually they are relatively small. Pits may be isolated from each other on the surface or so close together that they resemble a roughened surface. Possible forms of the cross-sectional shape of pits are shown in Fig. 1 Every engineering metal or alloy is susceptible to pitting. Pitting occurs when one area of a metal becomes anodic with respect to the rest of the surface or when highly localised changes in the corrosive agent in contact with the metal, as in crevices, cause accelerated localised attack.

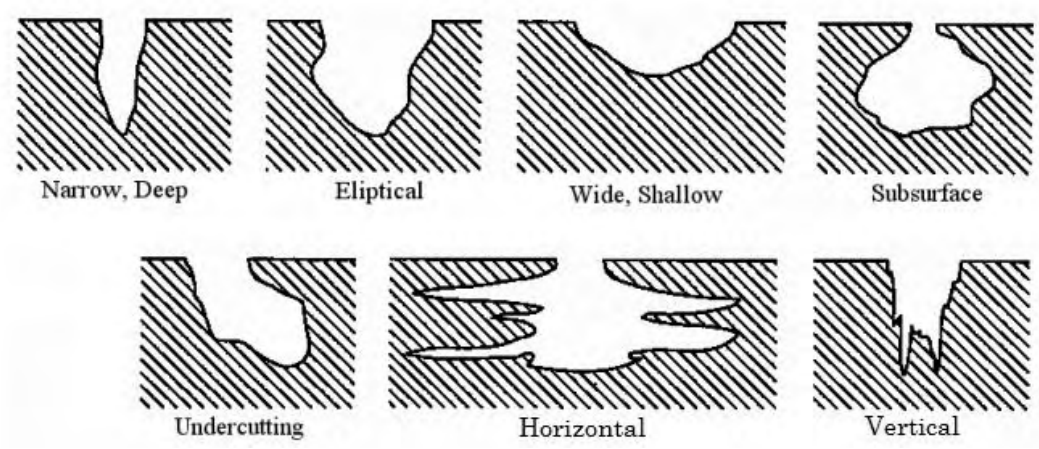

Figure 1 Various forms of pits

Pitting appears as one of the most insidious forms of corrosion. It can cause failure of materials by perforation while producing only a small weight loss on the metal. Pits are generally small and often remain undetected. A small number of isolated pits on a generally corrosion-free surface are easily overlooked. A large number of very small pits on a generally clean surface may not be detected by simple visual examination, or their potential for damage might be underestimated. [7]

2.2 Basic theory of steels

2.2.1 Phase diagram

The stable phases of steel have been discovered to vary with temperature and concentration of alloying elements, such as carbon. In a phase diagram, the stable phases are displayed as a function of both these variables. Figure displays an iron-carbon phase diagram, which is used most often as a simplification for the phase diagram of (low-alloyed) steel phase diagrams. It can be seen that for quite low carbon concentrations and temperatures, in between 400 and 900 °C, the iron is crystallised as BCC ferrite. For higher carbon contents, ferrite is stable until temperature A_{C1}, which is 727 °C in this case. Cementite (Fe_3C), a carbide of iron, is present in the ferrite when carbon content is higher, i.e. to the right of the right boundary of the ferritic phase, than the equilibrium content. When the temperature is increased above the A_{C1} temperature, FCC austenite will start to form. In Figure 1, a region can be observed in which both α and γ (ferrite and austenite) are present, called the intercritical region. The highest possible temperature in the intercritical region is the A_{C3} temperature which varies with carbon content; above this temperature, only austenite remains stable and the ferritic phase has been completely dissolved. For carbon contents higher than 2.14 wt% (depending of temperature), austenite will be in equilibrium with cementite.

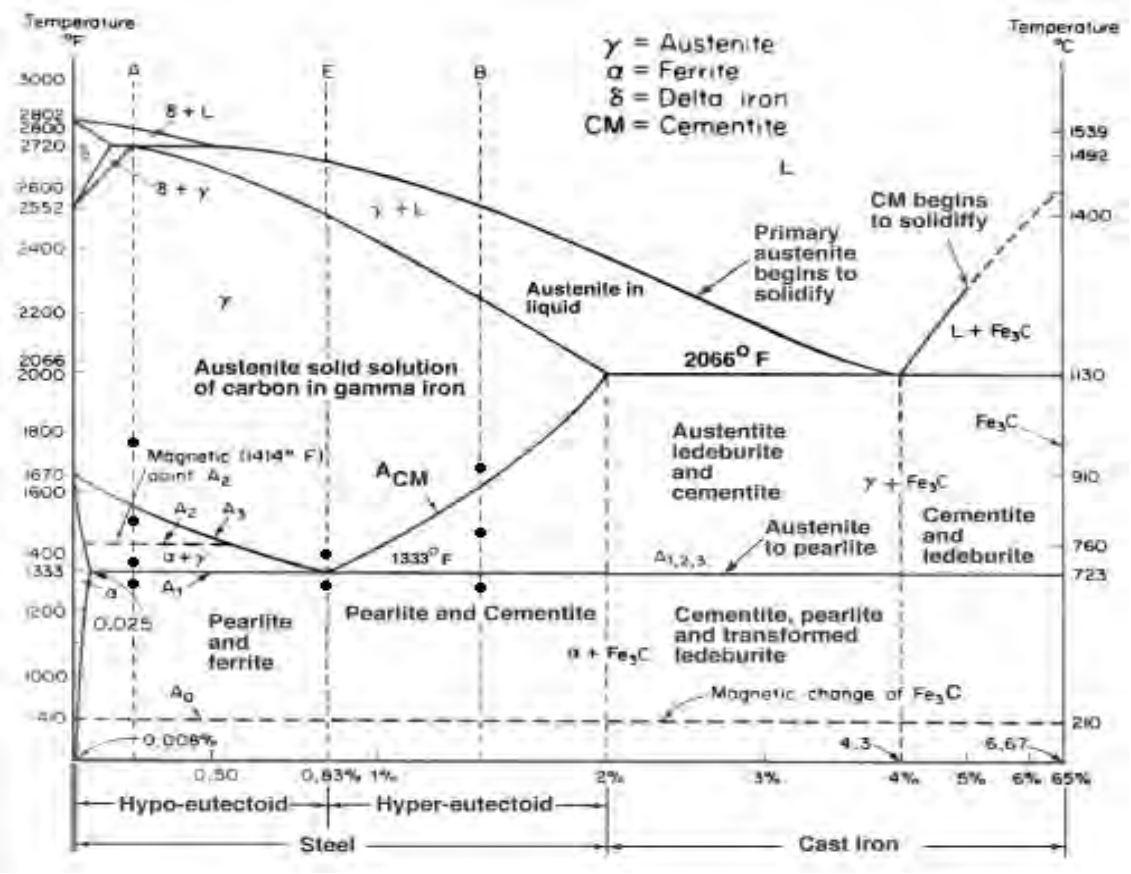

Figure 2 Fe-Fe_3C phase diagram showing the equilibrium phases and phase transformations per carbon mass content percent (%) for various temperatures [8]

2.2.2 Phase transformations

When steel is cooled from the γ towards the α phase, the newly formed ferrite phase needs to nucleate on the austenitic phase before it can expand. For the nucleation, a certain amount of undercooling below the equilibrium temperature is needed, because otherwise no driving force for nucleation is present. The growth of new amounts of phase is time-dependent, since nucleation is a probabilistic process and growth is neither instantaneous nor uniform. This means that by changing the cooling rate, the resulting microstructure can be altered. Nucleation of ferrite will generally occur at the boundaries of austenitic grains and triple points, because the energy level is higher at those places as compared to the bulk material; the

high energy level lowers the activation energy (EA) necessary for nucleation. Diffusion of alloying elements, such as carbon, will play a role during the growth of the new phase throughout the sample. The equilibrium carbon content (and that of other elements) in the intercritical region is lower for ferrite compared to austenite. Therefore, after the nucleation of ferrite, that surplus of carbon needs to be transferred from ferrite by diffusion, while ferrite is being formed. The timespan of diffusion is long enough when the cooling rate is sufficiently low and thus equilibrium behaviour, according to the phase diagram, may be expected. However, when the cooling rate increases, excess carbon can be trapped frozen in the matrix since diffusivity decreases rapidly with temperature and also diffusion timespan is shortened. When the sample is cooled from the austenitic region down to a temperature in the intercritical region, the separation of phases causes the microstructure to contain a fraction of ferrite and a fraction of austenite. It is obvious that the values of these fractions will vary for different annealing temperatures since the distances towards the boundaries of the ferritic and the austenitic regions will change, according to the lever rule. [9]

2.2.3 Transformation Induced Plasticity (TRIP) Steels

2.2.3.1 Fundamentals

TRIP steels constitute a category of innovative steels that feature a microstructure composed of ferrite, bainite and retained austenite, the latter transforming into martensite under appropriate conditions of stress or plastic strain. The ability of the austenitic phase (γ) to absorb a greater amount of energy, due to its transformation into martensite (a'), as the fraction of this phase increases [10], thus increasing the uniform elongation and formability, has contributed to the popularity of

TRIP steels with the car industry and to a increased interest about their capabilities.

The microstructure used to produce TRIP steels is usually ferritic-pearlitic before processing. The material is normally annealed for a specific period in the intercritical region $(\alpha + \gamma)$; above temperature A_{C1}, when pearlite rapidly dissolves into austenite and ferrite starts slowly transforming into austenite, and below $A_{C3,}$ where austenitisation is completed, and then cooled into the bainitic region where isothermal bainitic transformation (IBT) takes place and bainite (α_B) is formed with the simultaneous enrichment of austenite with carbon ejected from the bainitic phase. According to the desirable bainitic volume fraction, steel is then cooled to ambient temperature with the stabilised austenite remaining after the cooling forming a phase known as retained austenite (γ_R).

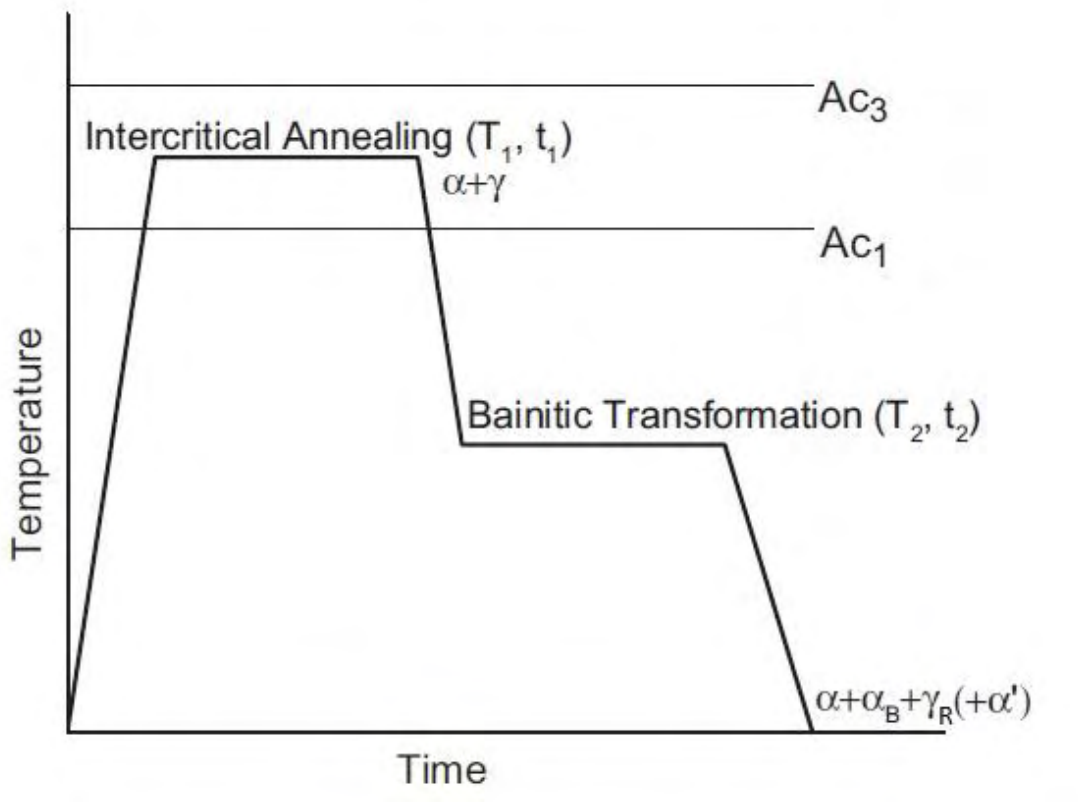

Figure 3 Schematic depiction of the generic heat treatment applied for the creation of TRIP steels

2.2.3.2 Heat treatments of TRIP steels

Heat treatments include all processes of controlled heating and cooling of steels for the change of their microstructure and a simultaneous creation of desirable properties. Relaxation of remaining stresses, homogenisation of alloying elements throughout the microstructure, softening, increase of yield stress or improvement of protection against wear and corrosion lie among the basic reasons for the thermal processing of steels.

Specific thermal treatments related to TRIP steels include::

Intercritical annealing, during which steel is heated in the region $\alpha+\gamma$ in order to create an admixture of austenitic and ferritic microstructure. It is frequently followed by abrupt

cooling into the bainitic region and an isothermal bainitic transformation (IBT) for the ultimate creation of a TRIP steel microstructure.

Austempering, a process of austenitisation and subsequent cooling down to the bainitic region so that the isothermal bainitic transformation can take place. This thermal process is an inherent part of the creation of TRIP steels, which may combine satisfactory strength and ductility. Silicon (Si) is often added as an alloying element because in sufficient quantities it can reduce or totally suspend the formation of cementite in the bainitic phase [11], with carbon instead enriching the austenitic phase and rendering it stable at room temperature.

2.2.3.3 Corrosion of TRIP steels

Bagdhasarian and Ravitz [12] mentioned early on the superior corrosion resistance of some TRIP steels against common stainless steels, such as 304 steel, in varying conditions, while also focusing on the effect that the amount of alloying elements like molybdenum have on corrosion behavior.

Later, the field of research expanded to investigate the interaction of corrosion with other modes of stress and failure, like corrosion fatigue or stress corrosion cracking [13] with quite satisfactory results of immunity for some TRIP steels.

Latest research focuses on increasingly detailed and innovative aspects of possible protection against corrosion, such as the influence of rare elements [14] and their action as corrosion inhibitors and attempts to create quantitative and qualitative correlations between corrosion properties and microstructure [15] or even tripartite correlation among corrosion, heat treatments and microstructure [16]. Also, potentiodynamic tests and SEM techniques have become increasingly useful as standard methods to evaluate the corrosion resistance of various multiphase TRIP steels.

2.2.4 Bainite

The term *bainite* refers to the microstructure that forms isothermally at temperatures above the M_s and below that required for formation of ferrite and pearlite, or in the case of cooling rates too rapid for the nucleation of these other transformation products, which require a fairly slow rate of cooling resembling equilibrium cooling conditions, but not rapid enough to elicit the formation of martensite. Conventionally, the morphology of bainite consists of two different types, namely the *upper bainite* and the *lower bainite*. These terms are due to structural differences noticed after isothermal transformation and may have little relevance to structures developed during continuous cooling. [17]

Upper bainite is formed in two stages. In the first stage, thin platelets of bainitic ferrite are nucleated and developed, with carbon being simultaneously transferred to austenite and cementite then precipitating between the ferritic platelets. The microstructure then expands to form aggregates of parallel ferritic platelets, known as bainitic sheaves, with cementite (Fe3C) particles between the sheaves.

Lower bainite forms at a lower temperature span, roughly 250-400 °C, and differs from upper bainite mainly because lower bainite also includes precipitation of cementite in the ferritic plates. In lower bainite ,the carbides are contained within the ferritic plates. In hypoeutectoid steels the ferrite platelets are formed first. [18]

3. Materials and Experimental procedure

3.1 Material

The original material used for all experiments was cold rolled TRIP 700 steel containing 0,202 wt% carbon, classified into the

broad category of low alloy steels, as the total mass of the alloying elements contained in it accounts for only about 3,7% of the total mass of the material. The steel sheet has a nominal thickness of 1mm.

The as received steel was provided by its manufacturer Voestalpine with the following chemical composition:

Element	**Fe**	**C**	**Si**	**Mn**	**P**
Mass Percentage %	balance	0,202	0,348	1,99	0,009

Element	**Al**	**S**	**Cr**	**Ni**	**Mo**
Mass Percentage %	1,07	0,0013	0,0038	0,017	0,011

Element	**Cu**	**W**	**As**	**Nb**	**Ti**
Mass Percentage %	0,044	0,02	0,004	0,002	0,002

Table 1 Chemical composition of the "as received material" in terms of mass composition

The as received steel contains 15,8 wt% retained austenite. The temperature above which austenitisation commences, A_{C1} , and that above which austenite is the only phase present, A_{C3} , were 673,85 °C and 913,43 °C respectively. Before being submitted to the selected heat treatments, specimens of the as received steel were first heated in the austenitic region at 950 °C for 4 minutes, with preheating at 280°C, then left to cool smoothly. This stage was used to ensure that all specimens would be subjected to heat treatments starting from a common inaugural state.

The details of the various heat treatments applied on the TRIP 700 steel are demonstrated in Table 2; the four thermal

treatments and the corresponding materials that are formed by them are listed and given the alphabetical symbols A to D.

At a first stage, all steel samples were heated to 890 °C and remained at that temperature for 60 seconds, to produce a mixture of austenite and ferrite. The steel was then cooled below 500 °C for the formation of bainite. During the isothermal bainitic transformation, austenite becomes enriched in carbon due to the transfer of carbon from the forming bainite to austenite. The thermal processes comprised also isothermal bainitic transformation at two different set temperatures, 400 °C and 460 C, and two differing hold timespans for each of these temperatures in the bainitic region.

Symbol of Material	Preheating	IA	IBT
A	400 °C, 120 s	890 °C, 60 s	400 °C, 120 s
B	400 °C, 120 s	890 °C, 60 s	400 °C, 820 s
C	400 °C, 120 s	890 °C, 60 s	460 °C, 120 s
D	400 °C, 120 s	890 °C, 60 s	460 °C, 820 s

Table 2 Characteristic details of the four different heat treatments

Data on the mass fraction of retained austenite for specific conditions are listed in Table 3.

Duration of IBT	120 s	820 s
Retained austenite %	14,8	12

Table 3 Percent of retained austenite for materials A and B

3.2 Test specimens and corrosion testing

The specimens used for the laboratory corrosion tests had dimensions of 40x15x1 mm in size. Two specimens were cut from each material including the original and the materials by heat treatment.

All specimens used for the immersion in the corrosion tank were prepared according to G1 Standard Practice [19] by ASTM. Each specimen was degreased by immersion in acetone and immediately afterwards thoroughly rinsed with deionised water. They were then smoothly dried by hot air blast and stored in dry conditions.

The corrosion experiments involved submersion of the TRIP steel specimens in aqueous solutions of sodium chloride 3,5% (NaCl). For the selection of the proper procedure for the corrosion test, specification ASTM G44 [20] was followed.

After being cut, cleaned and dried, the samples were immersed in a solution of NaCl in deionised water containing 3,5 % wt NaCl. The specimens were immersed for periods of 24 and 48 hours respectively in the corrosion solution.

Concerning the solution, the humidity, temperature and minimum volume qualifications stipulated in ASTM G44 were met during the corrosion immersion tests, with average 40% relative humidity and ambient temperature at 27±1 °C. Air circulation conditions were also compliant with the general guidelines of ASTM G44, to allow for non-stagnant air conditions.

With the completion of the immersion tests, all samples were removed from the solution, well rinsed with deionised

water to halt the corrosion process and weighed on a digital chemical scale to evaluate the mass loss due to corrosion.

3.4 Microscopy

After the completion of corrosion tests, smaller samples which were cut from the corroded specimens were prepared in order to be used for optical microscopy. A quickly solidifying and semi-transparent Struers mounting resin was used to embed the specimens into samples to be examined using optical microscopy. The embedding method contributed to the better handling and stability of the samples during metallographic processes.

Afterwards, the embedded specimens underwent manual wet grinding with grit 80, 320, 500, 800 and 1000 SiC papers. Between different grinding papers, samples were flushed with deionised water and ethanol to sweep away dirt and prevent further surface corrosion. When a smooth and satisfactorily scratch-free surface was achieved, all samples were polished using diamond particle-based slurry, with 3µm particles.

A Leitz Aristomet optical microscope was then employed for the examination of the specimens. To observe the results of the immersion experiments on the samples, the concealed internal cross-section of the samples had to be investigated. As the polished samples did not display any features of the microstructure under the microscope besides the shiny polished surface. Therefore, the polished samples needed to be etched to reveal the grains of the different phases. With an etchant, certain features like phases and grain boundaries are corroded to allow distinguishing one from another. An etchant is generally an acid. Before etching, the samples were rinsed with deionised water and ethanol to remove potential build-up dirt from polishing and then dried with hot-air draft.

To render the microstructure visible in the microscope, all embedded samples were etched with Nital 2% v/v solution, that is a solution of 2% v/v nitric acid dissolved in ethanol, to reveal grain boundaries and 10% v/v sodium metabisulphite ($Na_2 S_2O_5$) aqueous solution for 15 seconds to reveal the characteristics of each distinct phase of the microstructure.

Every etching substance was either instilled through dripping on the metal surface or the metal surface was gently slightly submerged into the liquid etchant. The main working principle of an etching medium is based on its preferential attacks to high-carbon regions. This duration was chosen as an optimal timespan of etching after a few trial-and-error efforts on a dummy sample. Finally, the samples were rinsed with ethanol again to remove any etchant residues.

With the microstructure visible, the samples were put under the lens of the optical microscope and photos were taken of the external interface of the metal surfaces of the samples in magnifications of 500 and 1000 times. Preferentially, corrosion pits were detected and photographed along with their surrounding microstructure.

4. Results

4.1 Mass variation

In Fig. 4,5 and 6, the decrease in mass due to corrosion is shown for every different immersion time as a fraction of the original mass of each specimen before the immersion. The results referring to the as received specimens are displayed in a separate chart for practicality, due to their large order of magnitude compared to the other specimens.

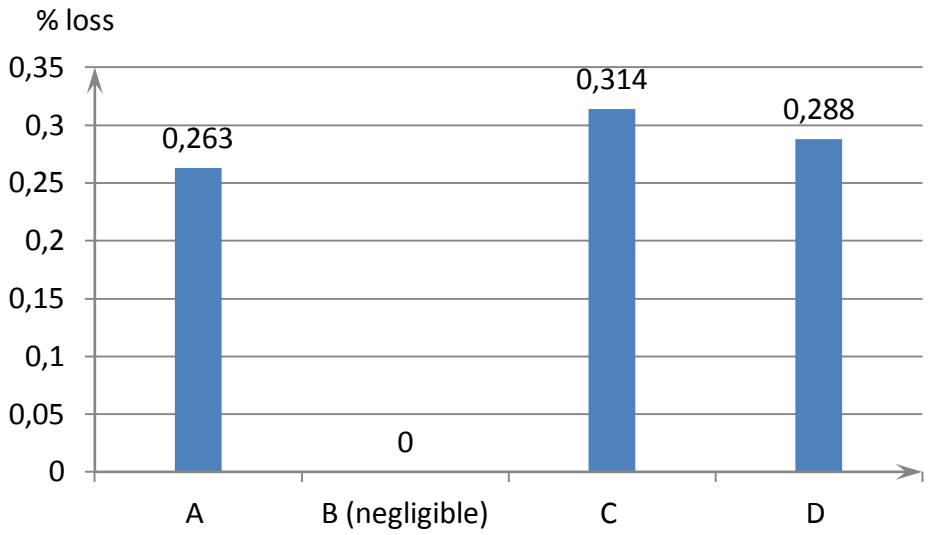

Figure 4 Mass loss percent (%) in A,B,C and D specimens for 24-corrosion

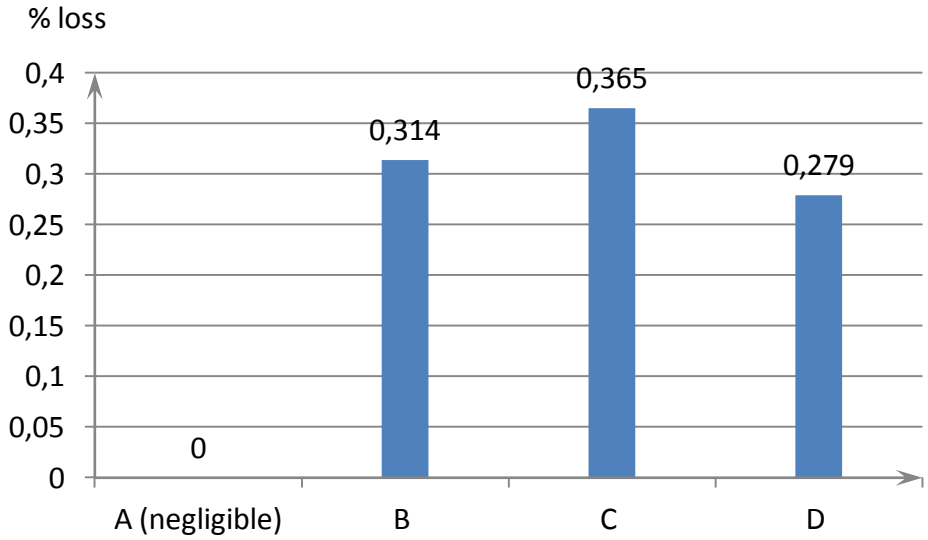

Figure 5 Mass loss percent (%) in specimens A,B,C and D specimens for 48h-corrosion

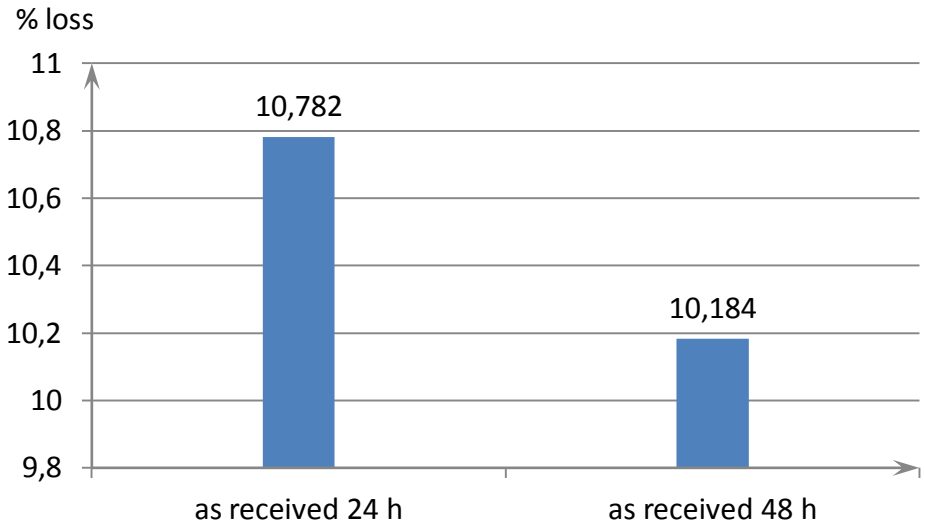

Figure 6 Mass loss percent (%) in as received specimens

4.2 Microscopical results

Photos were taken of the microstructures of all steels samples and measures were conducted on magnified pictures of the samples to obtain certain characteristics of the corrosion pits observed in the samples.

4.2.1 Microstructure

In Figures 7, 8 and 9, photographs from the microstructure of selected samples are shown. The scale of measurement is features inside the figures in micrometres (μm).

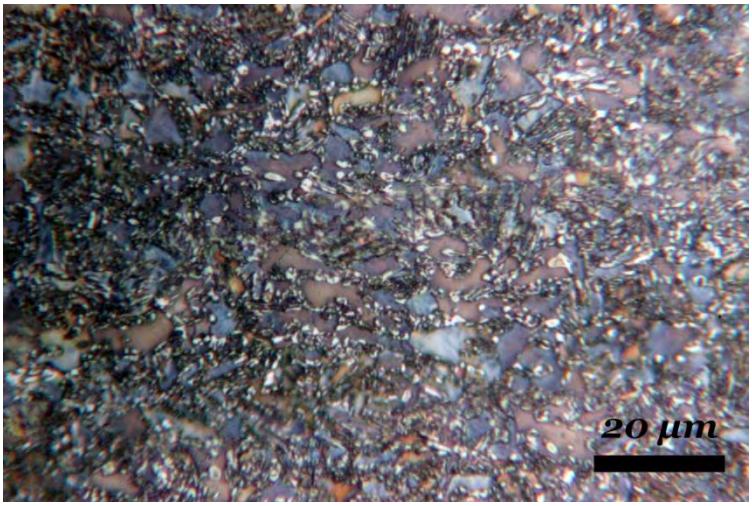

Figure 7 Microstructure of steel A for 24-hour corrosion, magnified 1000 times and etched with Nital and sodium metabisulphite

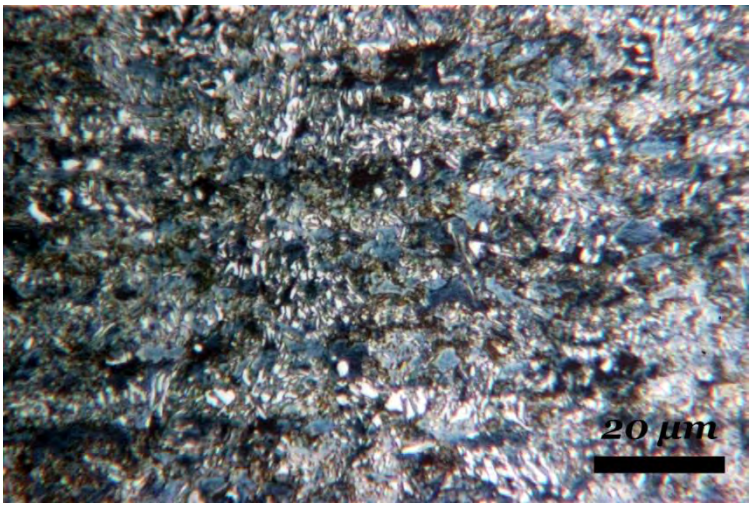

Figure 8 Microstructure of steel D for 48hour corrosion, magnified 1000 times and etched with Nital and sodium metabisulphite

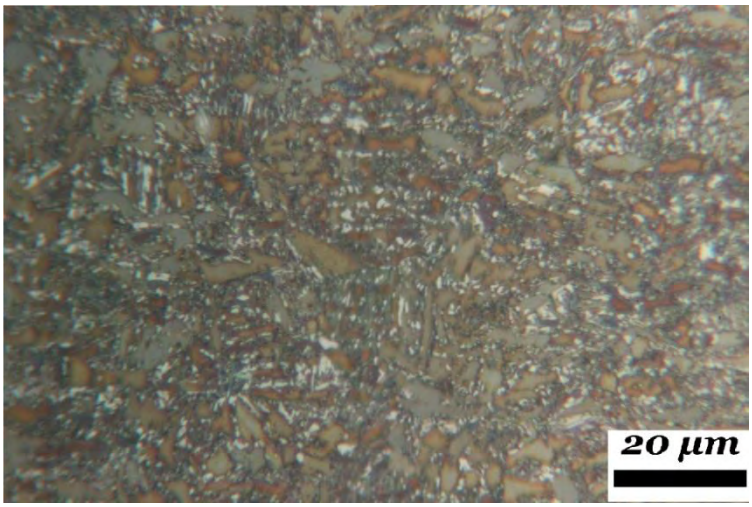

Figure 9 Microstructure of steel B for 24-hour corrosion, magnified 1000 times and etched with Nital and sodium metabisulphite

4.2.2 Pit measurements

With the use of the optical microscope, each sample was examined to obtain information about the size of corrosion pits on its surface. In Figures 10-14, a selected photos of a pit is shpown for every different steel A, B, C, D and the as received steel.

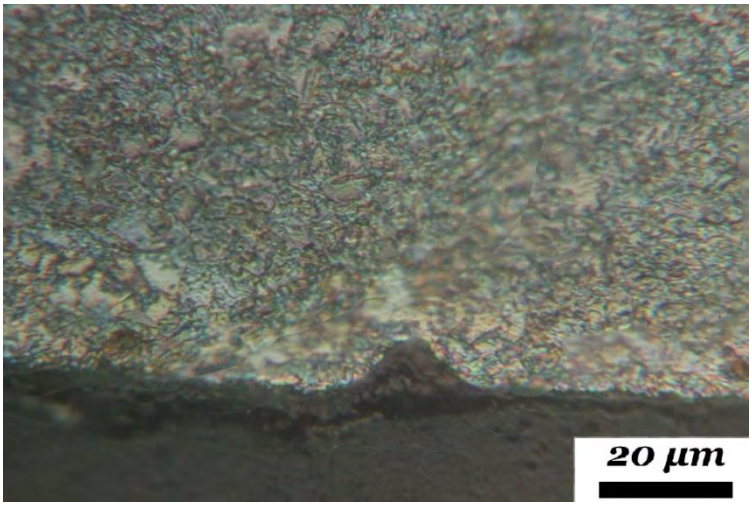

Figure 10 Pit in the as received steel for 24-hour corrosion

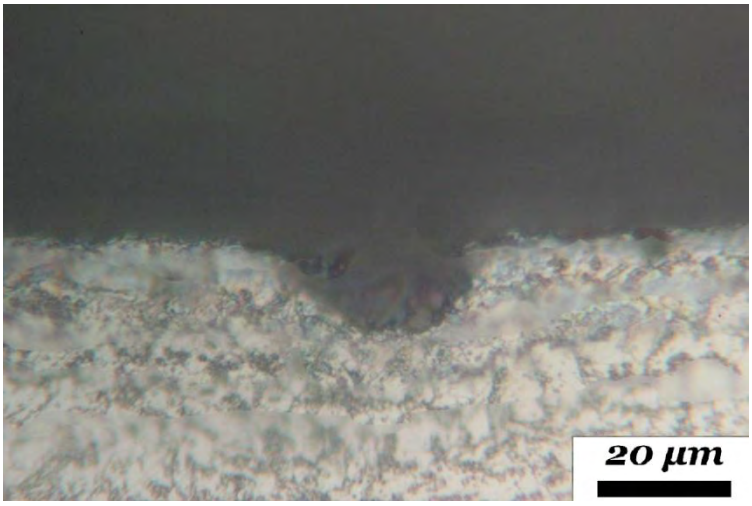

Figure 11 Pit in steel A for 48-hour corrosion

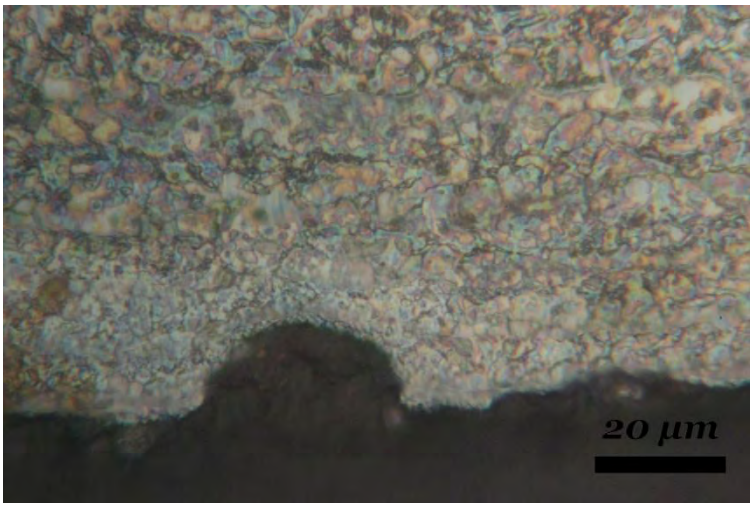

Figure 12 Pit in steel B for 48-hour corrosion

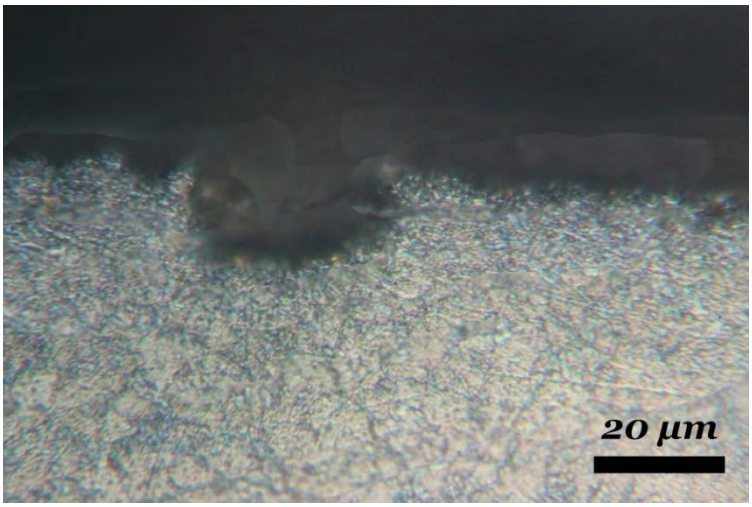

Figure 13 Pit in steel C for 24-hour corrosion

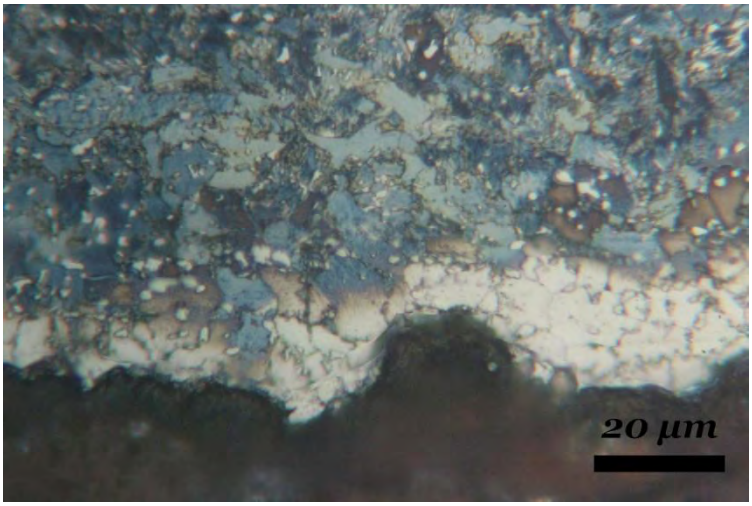

Figure 14 Pit in steel D for 48-hour corrosion

On the outer interface of the cross-section of each sample, the depth and width of a certain amount of pits formed due to corrosion were measured with the application of a Canon photographic camera attached to the lens of the microscope. Through these two quantities, it was possible to calculate the aspect ratio, that is the *depth to width ratio*, of the pits. All data were employed for the calculation of the respective average measures for each sample from the four heat treated materials

and the two corrosion times. All measured pit data are summarised in Tables 5-14.

4.2.2.1 As received material

DEPTH (µm)	WIDTH (µm)	ASPECT RATIO
9,29	17,85	0,52
9,64	25	0,39
7,15	11,43	0,63
7,86	21,43	0,37
5	12,14	0,41
4,29	9,3	0,46
MEAN	**MEAN**	**MEAN**
7,21	**16,19**	**0,46**

Table 4 Pit measurements obtained from as received steel for 24-hour corrosion

DEPTH (µm)	WIDTH (µm)	ASPECT RATIO
10,43	23,48	0,44
8,8	17,4	0,51
8,5	27,14	0,31
4,29	37,86	0,11
7,14	7,15	0,1
11,3	28,57	0,4
MEAN	**MEAN**	**MEAN**
8,41	**23,6**	**0,31**

Table 5 Pit measurements obtained from as received steel for 48-hour corrosion

4.2.2.2 Heat treatment A

DEPTH (µm)	WIDTH (µm)	ASPECT RATIO
10,71	35,71	0,4
14,29	35,71	0,4
12,86	17,86	0,72
12,14	32,14	0,38
5	21,43	0,23
10,72	19,29	0,56
MEAN	**MEAN**	**MEAN**
10,95	**27,02**	**0,45**

Table 6 Pit measurements obtained from A steel for 24-hour corrosion

DEPTH (µm)	WIDTH (µm)	ASPECT RATIO
17,86	39,29	0,45
13,57	27,14	0,5
7,14	10,71	0,67
7,1	19,29	0,37
10	30,71	0,33
32,14	50	0,64
MEAN	**MEAN**	**MEAN**
14,64	**29,52**	**0,49**

Table 7 Pit measurements obtained from A steel for 48-hour corrosion

4.2.2.3 Heat treatment B

DEPTH (µm)	WIDTH (µm)	ASPECT RATIO
10,7	42,86	0,25
14,28	32,86	0,43
8,57	32,14	0,27
3,57	14,29	0,25
5,71	19,28	0,30
5,8	17,14	0,34
MEAN	**MEAN**	**MEAN**
8,11	**26,43**	**0,31**

Table 8 Pit measurements obtained from B steel for 24-hour corrosion

DEPTH (µm)	WIDTH (µm)	ASPECT RATIO
19,29	46,43	0,42
12,14	32,17	0,38
12,86	30,36	0,42
7,13	25,71	0,28
8,57	20,74	0,41
12,92	39,28	0,33
MEAN	**MEAN**	**MEAN**
12,15	**32,45**	**0,37**

Table 9 Pit measurements obtained from B steel for 48-hour corrosion

4.2.2.4 Heat treatment C

DEPTH (µm)	WIDTH (µm)	ASPECT RATIO
5,7	10,71	0,53
17,86	35,7	0,5
14,29	32,14	0,44
9,3	12,9	0,72
14,26	18,61	0,77
8,6	28,6	0,3
MEAN	**MEAN**	**MEAN**
11,67	**23,11**	0,54

Table 10 Pit measurements obtained from C steel for 24-hour corrosion

DEPTH(µm)	WIDTH(µm)	ASPECT RATIO
14,29	21,43	0,67
20,71	35,7	0,58
10,7	17,14	0,62
15,7	16,8	0,93
9,28	30	0,31
12,84	32,15	0,4
MEAN	**MEAN**	**MEAN**
13,92	**25,54**	**0,59**

Table 11 Pit measurements obtained from C steel for 48-hour corrosion

4.2.2.5 Heat treatment D

DEPTH (µm)	WIDTH (µm)	ASPECT RATIO
5,7	14,64	0,39
8,57	26,43	0,32
7,86	23,6	0,33
10	21,4	0,47
7,5	18,6	0,40
5	7,86	0,64
MEAN	**MEAN**	**MEAN**
7,44	**18,76**	**0,43**

Table 12 Pit measurements obtained from D steel for 24-hour corrosion

DEPTH(µm)	WIDTH(µm)	ASPECT RATIO
12,14	23,5	0,52
13,57	24,3	0,56
14,3	32,14	0,44
15,71	29,28	0,54
18,6	33,57	0,55
11,07	23,6	0,47
MEAN	**MEAN**	**MEAN**
14,23	**27,73**	**0,51**

Table 13 Pit measurements obtained from D steel for 48-hour corrosion

4.3 Statistical calculations

Based on the microscopical measurements, average values were organised into bar charts, shown in Figures 15-20, for easier handling of the microscopical results and for a more concise and

useful display. Table 15 uses the results of the bar charts and shows the percent (%) difference in the average pit depth and width between 24 and 48-hour corrosion.

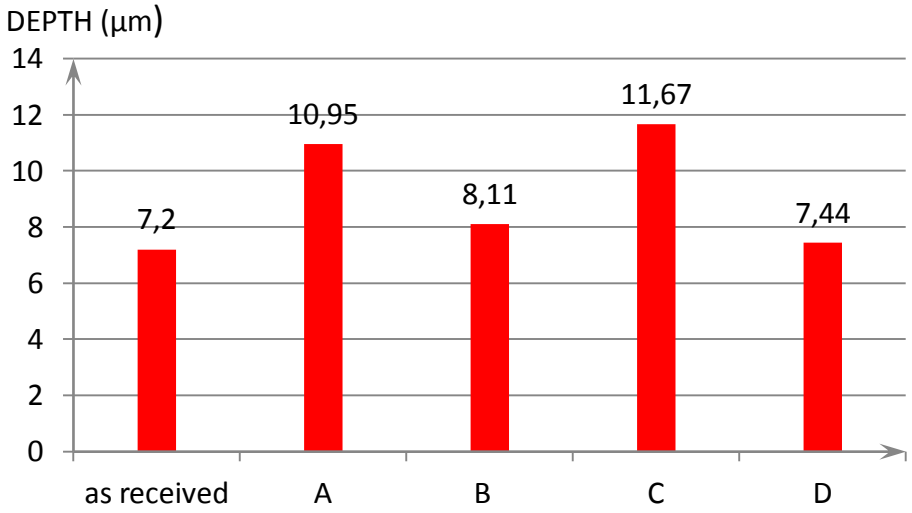

Figure 15 Average pit depth in steel samples for 24-hour corrosion

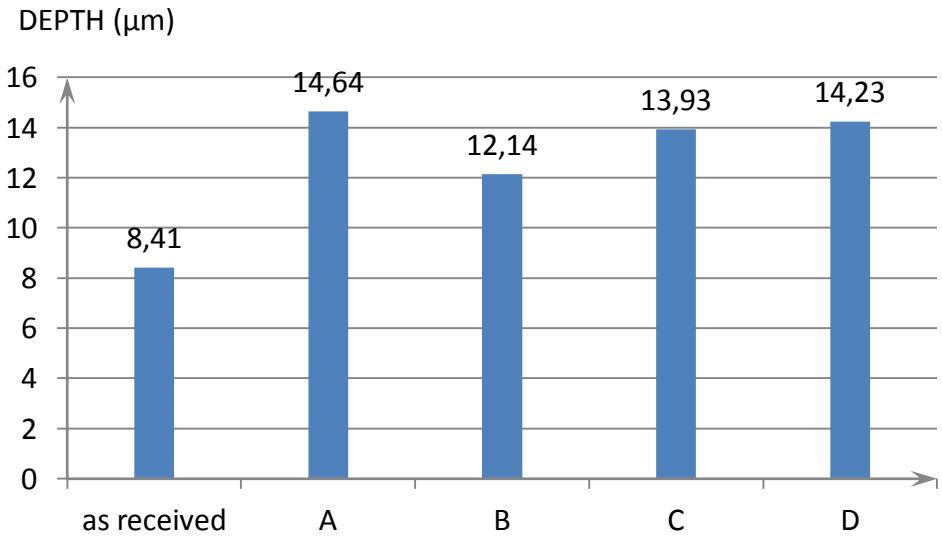

Figure 16 Average pit depth in steel samples for 48-hour corrosion

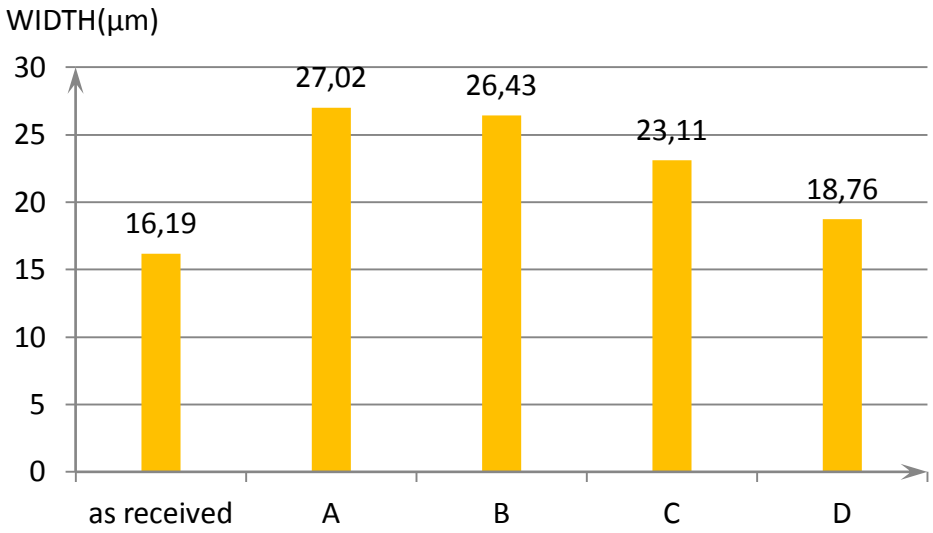

Figure 17 Average pit width in steel samples for 24-hour corrosion

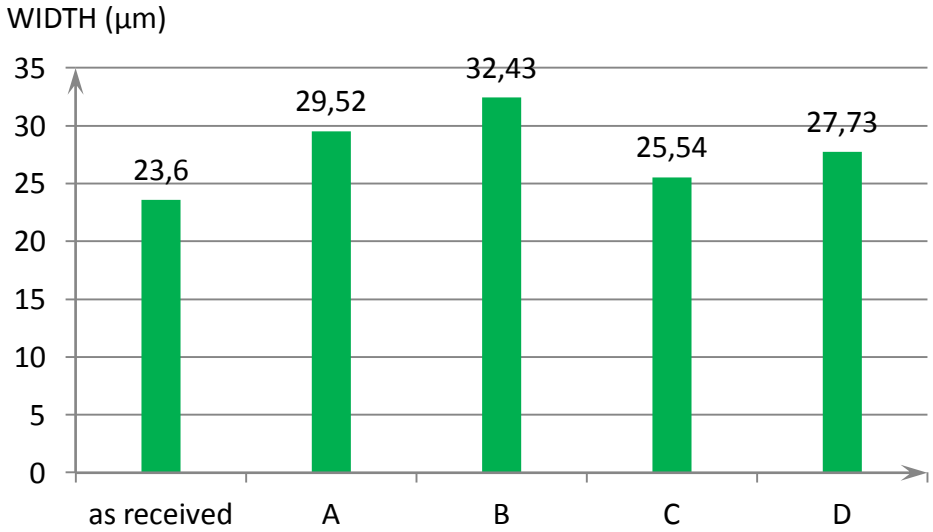

Figure 18 Average pit width in steel samples for 48-hour corrosion

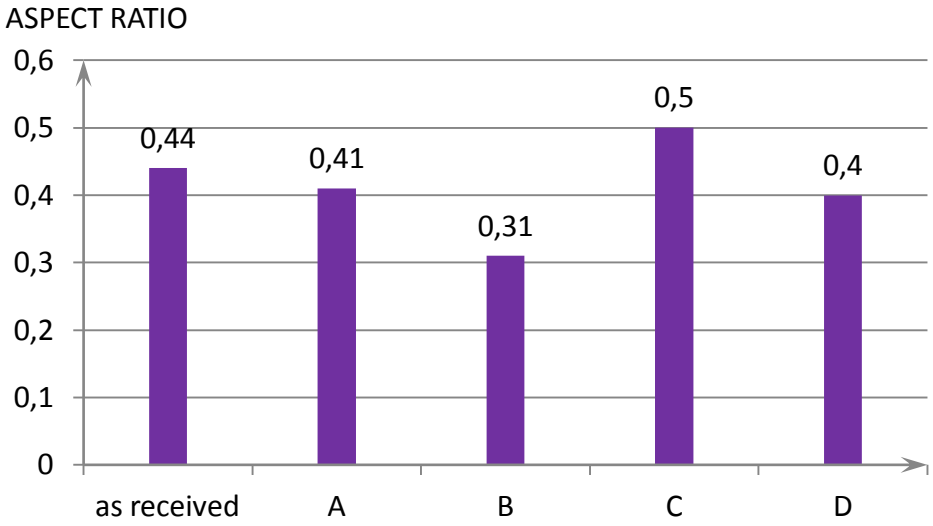

Figure 19 Average aspect ratio in steel samples for 24-hour corrosion

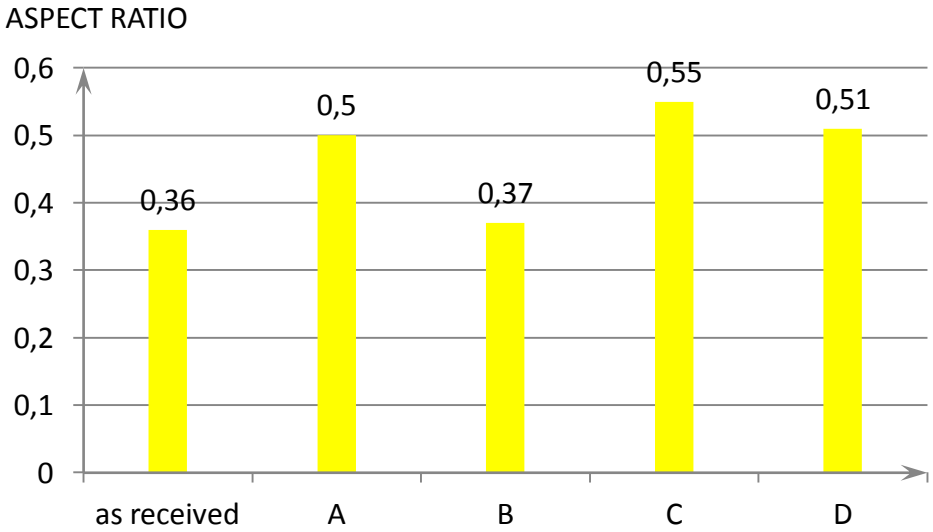

Figure 20 Average aspect ratio in steel samples for 48-hour corrosion

Relative difference	untreated steel	A	B	C	D
Depth (D)	0,168	0,337	0,497	0,194	0,913
Width (W)	0,458	0,092	0,227	0,105	0,478

Table 14 Relative difference in average pit depth, pit width and aspect ratio between 24 and 48 hour corrosion.

5. Discussion & Analysis

From the performed pit measurements it may be observed that the as received TRIP 700 material shows the best corrosion behaviour by having the smallest localized corrosion attack after 24 and 48 hours with the lowest average pit depths . Steels A and C present the largest average pit depth after 24 hours (material C) and 48 hours corrosion (material A).

Regarding the width of pits, the untreated material exhibits the lowest values, while the heat treatment process has a negative effect by increasing the width of pits specifically in the case of steels A and B.

Concerning the aspect ratio of pits, except for the B material which systematically presented the lowest ratio the differences are very small between the other materials.

As for the variation in mass before and after corrosion, material C has the highest relative amount of loss in both corrosion times. In 24-hour corrosion, however, there is lower

deviation of loss percent between the materials than in the 48-hour corrosion.

The increase of pit size in the heat treated materials may be associated with the increase in bainite volume fraction as a result of the high temperature and prolonged holding in the bainitic transformation region. Bainite increases corrosion susceptibility as it may act more effectively as an anode compared to adjacent phases of the matrix in TRIP steels [21]. As it can be observed in the micrographs of the microstructures shown in Figures 3-12 the content of bainite increases with increasing temperature and time specifically in the heat treatment processes A, C and D, while in heat treatment B although a higher bainite content compared to the untreated material is observed, its levels are lower compared to the other heat treatments,

6. Conclusions

The role of heat treatment on the corrosion behaviour of an Al containing TRIP 700 steel has been experimentally assessed. The main findings of the work suggest that:

- Immersion of TRIP steel samples into 3.5 %wt NaCl solution for 24 and 48 hours corrosion results to localised corrosion attack in the form of pits in the material. The extent of attack depends on the heat treatment process of the TRIP steel and the associated microstructure.
- The mass variation results indicate that the formation of upper bainite at higher temperatures during a faster

timespan leads to more soluble corrosion products and consequently to higher loss of material.

- It is probable that the bainitic transformation at a higher temperature well into the range of upper bainite, and for a greater period of time, leads to an increased bainitic volume fraction and renders the steel more vulnerable to pit creation.
- The aspect ratio of pits in materials presents small variations and is influenced to a smaller extent by heat treatment compared to the depth and width parameters.

List of Figures

References

[1] V. Zackay, E. R. Parker, D. Fahr and R. Busch, *Trans. ASM. 60, 252,* 1967.

[2] S. Baik, S. Kim, Y. Jin and O. Kwon, "Effects of Alloying Elements on Mechanical Properties and Phase Transformation of TRIP Cold Rolled Steel Sheets," *SAE 2000 Transactions Journal of Materials & Manufacturing - V109-5,* 2000.

[3] S. Aden-Ali, A. Chamat, J. Gilgert, E. Petit, S. Dominiak, L. Schmitt, M. Gilles and Z. Azari, "Fatigue Resistance of Hot-dip Galvanized Hot-rolled and High-Silicon TRIP Steel".

[4] A. Talapatra, "Microstructure-corrosion property relationship of TRIP steels by ultrasonic testing," 2011.

[5] F. Heakal El-Haib, N. Tantawy and O. Shehta, "Influence of chloride ion concentration on the corrosion behavior of Al-bearing TRIP steels," *Materials Chemistry and Physics, 130,* pp. 743-749, 2011.

[6] F. El-Taib Heakal, O. Shehata and N. Tantawy, "Effects of Nb and Cr on the Corrosion Characterization of Al-Containing Transformation-Induced Plasticity Steels in Neutral Chloride Solutions," *CORROSION,,* vol. 67, no. 9, September 2011.

[7] J. R. Davis, Corrosion, Understanding the Basics, 2000.

[8] H. Pollack, Materials Science and Metallurgy, Prentice-Hall, 1988, 4th edition.

[9] T. Remmerswaal, "The influence of microstructure on the corrosion behaviour of ferritic-martensitic steel, Master Thesis," 2015.

[10] I. D. Choi, D. M. Bruce, S. J. Kim, C. G. Lee, S. H. Park, D. K. Matlock and J. G. Speer, "Deformation Behavior of Low Carbon TRIP Sheet Steels at High Strain Rates," *ISIJ International, Vol. 42, No. 12,* p. 1483–1489, 2002.

[11] J. Mahieu, J. Maki, B. De Cooman and S. Claessens, "Phase Transformation and Mechanical Properties of Si-Free C-Mn-Al Transformation-Induced Plasticity-Aided Steel," *Metallurgical and Materials Transactions A,* pp. 2573-2580, August 2002.

[12] A. Baghdasarian and F. Ravitz, "Corrosion Resistance of Trip Steels," *Corrosion,* 1975.

[13] R. L. Jones, S. S. Wing and B. C. Syrett, "Stress Corrosion Cracking and Corrosion Fatigue of Some Surgical Implant Materials In a Physiological Saline ENvironment," *CORROSION,* vol. 34, no. 7, pp. 226-236, July 1978.

[14] F. Rosalbino and G. Scavino, "Influence of cerium(III) ions on corrosion of TRIP 800 steel in hydrochloric acid solution," *Materials and Corrosion,* vol. 67, no. 12, pp. 1329-1335, 12 December 2016.

[15] A. Talapatra, J. Datta and N. Bandhyopadhyay, " Structure-Properties Relationship of TRIP-assisted Steels by Non-destructive Testing Method. Chemical and Materials Engineering, 1 , 18 - 27. doi:

10.13189/cme.2013.010103.," vol. 7, no. 4, 2013.

[16] A. Talapatra, N. Bandhyopadhyay and J. Datta, "Correlation between Heat Treatment, Microsatructure and Properties of Trip-Assisted Steels," *International Journal of Mechanical, Aerospace, Industrial, Mechatronic and Manufacturing Engineering,* vol. 7, no. 4, 2013.

[17] W. Leslie and E. Hornbogen, "Physical Metallurgy of Steels," in *Physical Metallurgy*, 4th ed., vol. II, R. W. Cahn and P. Haasen, Eds., 1996, pp. 1555-1620.

[18] G. N. Haidemenopoulos, Physical Metallurgy, Tziolas Publications, 2007.

[19] ASTM G1, "Standard Practice for Preparing, Cleaning, and Evaluating Corrosion Test Specimens".

[20] ASTM G44, "Standard Practice for Exposure of Metals and Alloys by Alternate Immersion in Neutral 3.5 % Sodium Chloride Solution," 2005.

[21] I.-J. Park, S.-T. Kim, I.-S. Lee, Y.-S. Park and M.-B. Moon, "A Study on Corrosion Behavior of DP-Type and TRIP-Type Cold Rolled Steel Sheet," *Materials Transactions, Vol. 50, No. 6,* p. 1440 to 1447, 2009.